ScientificScholar®
Knowledge is power
Publisher of Scientific Journals

www.surgicalneurologyint.com

Surgical Neurology International

Editor-in-Chief: Nancy E. Epstein, MD, Clinical Professor of Neurological Surgery, School of Medicine, State U. of NY at Stony Brook.

SNI: Pediatric Neurosurgery

Editor
Frank Van Calenbergh, MD
University Hospitals; Leuven, Belgium

SNI
Open Access

*Original Article*

# Surgical histopathology of a filar anomaly as an additional tethering element associated with closed spinal dysraphism of primary neurulation failure

Takato Morioka[1,2], Nobuya Murakami[1], Satoshi O. Suzuki[3], Nobutaka Mukae[4], Takafumi Shimogawa[5], Ai Kurogi[1], Tadahisa Shono[2], Masahiro Mizoguchi[4]

[1]Department of Neurosurgery, Fukuoka Children's Hospital, Fukuoka, [2]Department of Neurosurgery, Harasanshin Hospital, [3]Department of Psychiatry, Shourai Hospital, Karatsu, Saga, [4]Department of Neurosurgery, Graduate School of Medical Sciences, [5]Department of Neurosurgery, Kyushu University, Fukuoka, Fukuoka, Japan.

E-mail: Takato Morioka - takato@ns.med.kyushu-u.ac.jp; *Nobuya Murakami - murakami.n@fcho.jp; Satoshi O. Suzuki - sosuzuki@shouraikai.jp; Nobutaka Mukae - mukae@ns.med.kyushu-u.ac.jp; Takafumi Shimogawa - shimogawa28@gmail.com; Ai Kurogi1 - aironron8282@gmail.com; Tadahisa Shono - tadahisashono@gmail.com; Masahiro Mizoguchi - mmizoguc@ns.med.kyushu-u.ac.jp

***Corresponding author:**
Nobuya Murakami,
Department of Neurosurgery,
Fukuoka Children's Hospital,
Fukuoka, Japan.

murakami .n@fcho.jp

Received : 07 April 2021
Accepted : 09 June 2021
Published : 27 July 2021

**DOI**
10.25259/SNI_340_2021

**Quick Response Code:**

## ABSTRACT

**Background:** Closed spinal dysraphism of primary neurulation failure could be associated with filar anomalies, such as filar lipoma or thickened and tight filum terminale (TFT), resulting from impaired secondary neurulation. Retained medullary cord (RMC) is a remnant of the cavitary medullary cord originating from the secondary neurulation failure. Some filar lipomas are known to contain a central canal-like ependyma-lined lumen with surrounding neuroglial tissues (E-LC w/NGT), that is, a characteristic histopathology of RMC. To clarify the embryological background of these filar anomalies, we evaluated the histopathological findings.

**Methods:** Among 41 patients with lesions of primary neurulation failure who underwent initial untethering surgery, the filum including cord-like structure (C-LS) was additionally resected in 10 patients (five dorsal and transitional lipomas; five limited dorsal myeloschisis). We retrospectively analyzed the clinical, neuroradiological, intraoperative, and histopathological findings.

**Results:** Among 10 patients, two patients were diagnosed with RMC based on morphological features and intraoperative neurophysiological monitoring. The diagnosis of filar lipoma was made in six patients, since various amounts of fibroadipose tissue were histopathologically noted in the filum. Two patients were diagnosed with TFT, since the filum was composed solely of fibrocollagenous tissue. E-LC w/NGT was noted not only in both C-LSs of RMCs but also in two out of six fila both with filar lipomas and fila with TFTs.

**Conclusion:** These findings provide further evidence for the idea that entities, such as filar lipoma, TFT, and RMC, can be considered consequences of a continuum of regression failure occurring during late secondary neurulation.

**Keywords:** Central canal, Ependyma, Filar type lipoma, Neuroglial core, Primary neurulation, Retained medullary cord, Secondary neurulation

## INTRODUCTION

The central nervous system and vertebrae are formed during the neurulation process that occurs early in embryonic life and are responsible for the transformation of the flat neural plate into

the neural tube. Primary neurulation allows the formation of the brain and the spinal cord down to the junction between the S1 and S2 segments, whereas secondary neurulation is responsible for the formation of the spinal cord segments distal to the S1-2 junction. Although primary neurulation is relatively well understood, less is known about the process of secondary neurulation or its clinical importance.[15,20,21] It is generally speculated that secondary neurulation begins with mesenchymal epithelium transformation within a pluripotential blastema called the caudal cell mass or caudal eminence. A sequence of events then proceeds from the condensation of mesenchyme into a solid medullary cord to intrachordal lumen formation and eventual partial degeneration of the cavitary medullary cord until only the conus and filum remain.[7,20,21]

Failure of primary neurulation leads to open neural tube defects, including myelomeningocele and myeloschisis, or closed neural tube defects, including spinal lipoma of dorsal and transitional type, limited dorsal myeloschisis (LDM), and congenital dermal sinus (CDS). When the secondary neurulation process is impaired, the result is either a defect of formation that leads to an absent conus and a short spinal cord, a condition known as caudal agenesis,[22] or a defect during its regression, as we can see in the terminal myelocystocele, spinal lipoma of caudal and filar type, thickened and tight filum terminale (TFT), and retained medullary cord (RMC).[15,20,21]

RMC is a newly defined entity of closed spinal dysraphism that is thought to originate from an almost complete arrest of apoptosis during the last phase of secondary neurulation.[20,21] The morphological feature of RMC is a redundant nonfunctional cord-like structure (C-LS) continuous from the conus medullaris and extends to the dural cul-de-sac, which can produce neurological deficits by tethering.[7,10,18,20,21,25] As a nonfunctional RMC is indistinguishable from the functional conus on neuroimaging and in the intraoperative view, confirmation of the presence of a nonfunctional C-LS with intraoperative neurophysiological monitoring (IONM) is essential for the diagnosis of RMC.[7,9,10,20,21,23] Histopathology of the C-LS resected at surgery typically shows a central canal-like, ependyma-lined canal with surrounding neuroglial tissues (E-LC w/NGT), corroborating the picture of a remnant of the cavitary medullary cord, which is normally regressed but can remain due to late arrest of secondary neurulation before the degenerative phase.[20,21]

When there are alterations present in both the primary and secondary neurulation, we can find the coexistence of dysraphism that presents with elements from the two forms of neural tube defects.[8,9,15,21] While Gupta and Rajshekhar[4] stressed that closed spinal dysraphism of primary neurulation failure could be associated with filar anomalies, such as filar lipoma (or fatty filum) or TFT, resulting from impaired secondary neurulation, as an additional tethering element, detailed histopathological findings have not been fully demonstrated. Our previous report demonstrated that some filar lipomas also contain E-LC w/NGT, which is the characteristic histopathology of the C-LS of RMC.[16,19] To clarify the embryological background of these filar anomalies, we evaluated the histopathological findings, paying special attention to E-LC w/NGT.

## MATERIALS AND METHODS

From January 2015 to December 2020, 41 patients with closed spinal dysraphic lesions of primary neurulation failure underwent initial untethering surgery at Fukuoka Children's Hospital and related hospitals under supervision of the first author (T.M.). There were 16 spinal lipomas at the lumbosacral region (six dorsal lipomas and 10 transitional lipomas), 23 LDMs, and two CDSs with dermoid/epidermoid cysts. Split cord malformation, which is caused by developmental failure of the notochord, was not involved in the present study. At our institute, the classification of spinal lipoma was based on Arai *et al*.[1,11] Because lipomyelomeningocele based on Arai's classification is thought to result from failed neurulation between the primary and secondary stages (junctional neurulation),[15] lipomyelomeningocele was not included in this study.

In all patients, preoperative and postoperative magnetic resonance imaging (MRI), including three-dimensional T1-weighted spoiled gradient-recalled echo images or variable flip angle three-dimensional turbo spin echo T1-weighted images, and three-dimensional heavily T2-weighted images, were performed as described in our previous report.[5,17]

The decision to sever the filum was based on whether the filum was involved as an additional tethering element, judging from the preoperative MRI and intraoperative findings. Based on the intraoperative morphological findings, the fila were classified into three types; CL-S, fatty filum (short fatty filum, tight fatty filum, or fatty filum), and short or tight filum. Before cutting the filum, for IONM, we confirmed that no compound muscle action potentials (CMAPs) were evoked at the external anal sphincter, hamstrings, and gastrocunemius muscles following the stimulation of the filum to be severed. In cases of suspected RMC, the border between the true cord and nonfunctional C-LS was determined by tracing the evoked CMAPs by stimulation in the rostrocaudal direction, beginning from the functional cord, and proceeding to the nonfunctional C-LS, as described previously.[9,10]

Among these 41 patients, the filum was additionally resected in 10 patients. Of the six patients with dorsal lipomas, the filum was resected in Patient 1 [Table 1],

**Table 1:** Clinical and histopathological findings of five patients with dorsal and transitional lipoma and associated filar anomaly.

| | Preoperative MRI findings | | | | | | Intraoperative findings of filum | | Histopathological findings of filum | | | |
|---|---|---|---|---|---|---|---|---|---|---|---|---|
| Patient no | Age/ Gender | Skin findings | Type of lipoma | Spinal entry of lipoma | Location of conus | Filum diameter/ intensity | Appearance | IONM | E-LC w/ NGT | Fibro-adipose tissue | Fibro-collagenous tissue | Final diagnosis of filar anomaly |
| 1 | 2 months/F | Subcutaneous mass | Dorsal | L4-5 | L5 | 2 mm/ isointensity | C-LS continuous from conus | Determined border* | + | – | + | RMC |
| 2 | 4 months/F | Subcutaneous mass | Transitional | L5-S1 | L4 | 1 mm/ isointensity | Short filum | No CMAP | + | – | + | TFT |
| 3 | 3 years/F | Subcutaneous mass | Transitional | S1 | L5 | Not determined | Short filum | No CMAP | – | + (3:7) | + | Filar lipoma |
| 4 | 4 months/F | Tail-like appendage | Transitional | S1 | L5 | Not determined | Short fatty filum | No CMAP | – | + | – | Filar lipoma |
| 5 | 6 month/M | Tail-like appendage | Transitional | L5 | L3-4 | 1.5 mm/ Hyperintensity | Short fatty filum | No CMAP | – | + (8:2) | + | Filar lipoma |

MRI: Magnetic resonance images, IONM: Intraoperative neurophysiological monitoring, ELC w/NGT: Ependyma-lined canal with surrounding neuroglial tissues, M: Month; y: Year, F: Female, M: Male, C-LS: Cord-like structure, CMAP: Compound muscle action potentials, *The border between true conus and nonfunctional CL-S was determined with IONMy, (:): Ratio of the fibroadipose and fibrocollagenous tissues, RMC: Retained medullary cord, TFT: Tight filum terminale

since preoperative MRI and intraoperative findings demonstrated a low-lying conus medullaris, which was tethered by C-LS, extended from the conus and terminated at the dural cul-de-sac without much tapering, in addition to the dorsal lipoma. Of the 10 patients with transitional lipomas, the filum was resected in four patients (Patients 2-5), [Table 1], because the untethering procedure of the cord from the lipoma intraoperatively revealed that the cord was also tethered with a short or short fatty filum that was rarely demonstrated by preoperative MRI. Out of 23 LDM patients, the filum was resected in five patients (Patients 6-10), [Table 2]. The preoperative MRI demonstrated a low-lying conus, which was tethered by C-LS in Patient 6, tight filum in Patients 7 and 9, and fatty filum in Patients 8 and 10, in addition to LDM stalk. The detailed clinicopathological findings of LDM in Patients 6-10 have been described before [Table 2].[6,9,12-14]

In all patients, the filum was resected as a column and placed in formalin. Routinely prepared histopathological sections were stained with hematoxylin and eosin or immunostained for glial fibrillary acidic protein (GFAP) and S-100 protein as part of the standard diagnostic analysis. Histopathological examination was performed with particular attention to the presence or absence of fibroadipose tissue, fibrocollagenous tissue, and E-LC w/NGT. When fibroadipose and fibrocollagenous tissues were present, the ratio of both was visually determined. The final differential diagnosis of filar lipoma from TFT was made with the histopathological presence of fibroadipose tissue. In all 10 patients, no postoperative neurological worsening was noted. We retrospectively analyzed the clinical, neuroradiological, intraoperative, and histopathological findings of these 10 patients.

## RESULTS

On histopathological examination of the resected filum including C-LS, E-LC w/NGT was noted in two out of five patients (Patients 1 and 2) with dorsal [Figure 1a-g] and transitional lipomas [Figure 2], and in three out of five patients (Patients 7-9) with LDM [Figure 3a-e]. In Patient 6, there was no E-LC but NGT. We think that small islands of E-LC may have been missed during routine sectioning of the surgical specimen, as were described elsewhere;[9] hence, it was determined to be positive E-LC w/NGT. Thus, E-LC w/NGT was noted in 8 (66.7%) out of 10 fila, including C-LSs.

Among these eight patients with positive E-LC w/NGT, the final diagnosis of RMC was made in two patients (Patient 1 with dorsal lipoma and Patient 6 with LDM), based on the morphological features and IONM findings [Figure 1b-f]. In these two patients, E-LC w/NGT was noted in the marginal part of the fibrocollagenous tissue [Figure 1e-g]. On preoperative T1-weighted MRI, C-LS was demonstrated

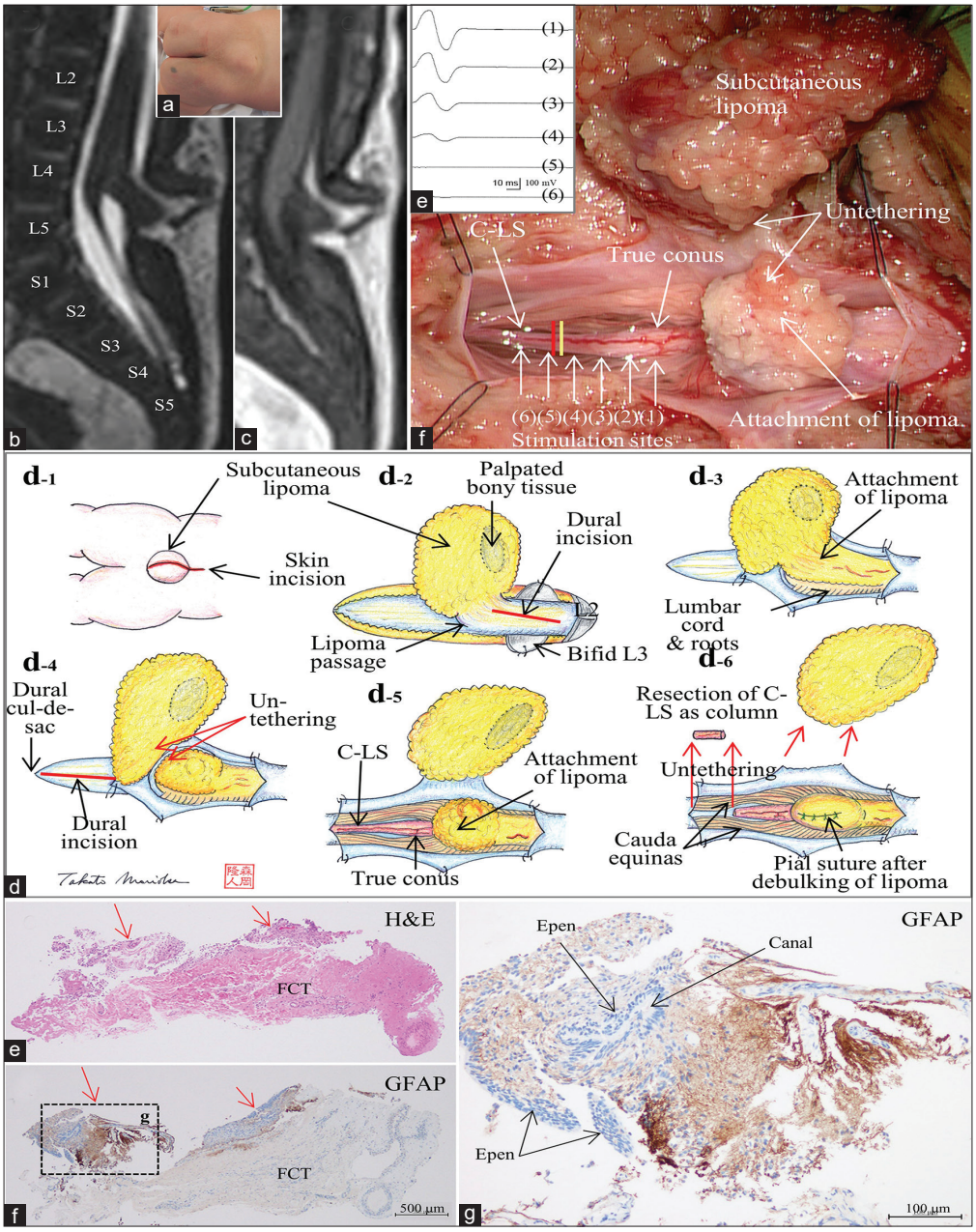


**Figure 1:** (Patient 1) (a) Photograph showing a subcutaneous lipoma at the lumbosacral region. Sagittal views of a three-dimensional heavily T2-weighted image (3D-hT2WI, slice thickness of 1.25 mm) (b) and a 3D variable flip angle T1-weighted image (3D-T1WI, slice thickness of 1.25 mm) (c) depict a low-lying conus medullaris at the vertebral level of L5 that is tethered by dorsal lipoma, and cord-like structure (C-LS) extends from the conus and terminates at the dural cul-de-sac at S4-5 level without much tapering. Schematic drawings (d) and microscopic view of the operative findings (e), and intraoperative neurophysiological monitoring (f). (d-1) A linear skin incision on the subcutaneous lipoma and a subsequent incision on the rostral side are made. (d-2) Passage of the lipoma through the dura mater is noted at L4 level, and the dura incision is made on the rostral site to the lipoma passage. (d-3) With the dura opened, the intradural component of lipoma is exposed. (d-4) Lumbar cord is untethered from the lipoma. The dura incision is made on the caudal site to the lipoma passage and extended to the dural cul-de-sac. (d-5, e) With the dura opened, C-LS is continuous from the conus to the dural cul-de-sac. The exact border between the C-LS and the true conus is determined by tracing the evoked compound muscle action potentials of the external anal sphincter muscle (f) with direct stimulation starting from the functional portion of the conus (1-4) and continuing to the nonfunctional portion of the C-LS (5 and 6), and indicated by the yellow line in (e). C-LS is severed immediately caudal to the exact border (indicated with red line in (e)). (d-6) Caudal end of the C-LS is also severed, and the C-LS is resected as column. Finally, the lipoma is debulked, and the pial surface is reconstructed with sutures. (e-g) Photomicrograph of longitudinal sections of the C-LS stained with hematoxylin and eosin (H and E) (e) and immunostained for glial fibrillary acidic protein (GFAP) (f and g). A higher magnification view of the area indicated by the dotted square in (f) is shown in (g). In the marginal part of the fibrocollagenous tissue of the C-LS, a central canal-like, ependyma (Epen)-lined canal with surrounding GFAP-immunopositive neuroglial tissues is noted (indicated with red arrows in (e) and (f)). No adipose tissue is noted.

**Table 2:** Clinical and histopathological findings of five patients with limited dorsal myeloschisis and associated filar anomaly.

| | Preoperative MRI findings | | | | | Intraoperative findings of filum | | Histopathological findings of filum | | | | | |
|---|---|---|---|---|---|---|---|---|---|---|---|---|---|
| Patient no | Age/ Gender | Skin findings | LDM Spinal entry/cord attachment | Location of conus | Filum diameter/ intensity | Appearance | IONM | E-LC w/NGT | Fibroadipose tissue | Fibrocollagenous tissue | Others | Final diagnosis of filar pathology | References |
| 6 | 2 months/M | Tail-like appendage/ dimple | T8/T8 | L3 | 1.5 mm/ isointensity | C-LS continuous from conus | Determined border* | – (NGT+) | – | + | Peripheral nerves | RMC | [11] |
| 7 | 5 years/F | Cigarette burn | S1-2/L4 | S1 | 1.5 mm/ isointensity | Tight filum | No CMAP | + | – | + | | TFT | Patient 4 in[19] |
| 8 | 7 months/F | Cigarette burn | L4/L3 | L5 | 2 mm/slight hyperintensity | Tight fatty filum | No CMAP | + | + (4:6) | + | | Filar lipoma | [18] |
| 9 | 1 day/F | Saccular lesion | L2/L1 | L4-5 | 1.5 mm/ isointensity | Fatty filum | No CMAP | + | + (3:7) | + | | Filar lipoma | Patient 1 in[21] |
| 10 | 2 years/6 month/F | Cigarette burn | S1/L3 | L3 | 1.5 mm/ hyperintensity | Fatty filum | No CMAP | – | + (8:2) | + | | Filar lipoma | Patient 5 in[22] |

MRI: Magnetic resonance images, LDM: Limited dorsal myeloschisis, IONM: Intraoperative neurophysiological monitoring, E-LC w/NGT: Ependyma-lined canal with surrounding neuroglial tissues, m: Month, y: Year, F: Female, M: Male, C-LS: Cord-like structure, CMAP: Compound muscle action potentials, *: The border between true conus and nonfunctional cord or filum was determined with IONM, *: Associated with split cord malformation type II; (:): Ratio of the fibroadipose and fibrocollagenous tissues

as isointensity, with a diameter of 2 mm in Patient 1 and 1.5 mm in Patient 6.

The final diagnosis of filar lipoma was made in eight patients (Patients 3-5 with transitional lipoma and Patients 8-10 with LDM), since various amounts of fibroadipose tissue were histopathologically noted in the filum. There was only one filum in Patient 4 composed solely of fibroadipose tissue; however, the remaining seven patients had a mixture of fibroadipose and fibrocollagenous tissues. When the ratio of fibroadipose and fibrocollagenous tissues was 4:6 or more, the filum was demonstrated as high intensity on T1-weighted MRI and looked like fatty filum in the intraoperative view. However, when the ratio was 3:7, the filum was demonstrated as isointensity on T1-weighted MRI, as seen in Patient 9 [Figure 3c and d] and did not look like a fatty filum in the operative view, as seen in Patient 3. On preoperative MRI, the diameter of the filar lipoma was 1.5 mm in three patients and 2 mm in two patients. In Patients 3 and 4, who had transitional lipoma, the filum was not demonstrated on MRI. In six filar lipomas, two patients (Patients 8 and 9 with LDM) had E-LC w/NGT in the fibroadipose tissue with various amounts of fibrocollagenous tissue [Figure 3d and e].

In the remaining two patients (Patient 2 with transitional lipoma and Patient 7 with LDM), the final diagnosis of TFT was made, since the filum was composed solely of dense fibrocollagenous tissue without fibroadipose tissue [Figure 2]. On preoperative MRI, the TFT was isointense with a diameter of 1 mm in Patient 2 and 1.5 mm in Patient 7. Both TFT had E-LC w/NGT in the fibrocollagenous tissue [Figure 2].

## DISCUSSION

In this study, E-LC w/NGT was histopathologically observed in 6 (60%) out of 10 fila, including C-LSs, which were resected, as an additional tethering element, in 41 patients with closed spinal dysraphism of primary neurulation failure. However, the histopathological confirmation of E-LC w/NGT alone does not lead to the diagnosis of RMC, and the IONM confirmation of the functional conus and nonfunctional C-LS is essential.[7,9,20,21,23] Kim *et al.*[7] proposed the term "possible RMC," in which the presence of nonfunctional C-LS could not be confirmed by IONM because of limited operative exposure, but they also agreed that there may be an overuse or abuse of the term. In this study, the diagnosis of RMC could be made in two patients with dorsal lipoma or LDM. In the original description by Pang *et al.*,[21] one out of seven RMC patients had an LDM stalk that was attached to the dorsal cord, rostral to the conus, and RMC. Our finding provides further evidence for the coexistence of primary neurulation failure and RMC,[8,9] in addition to filar lipoma and TFT.

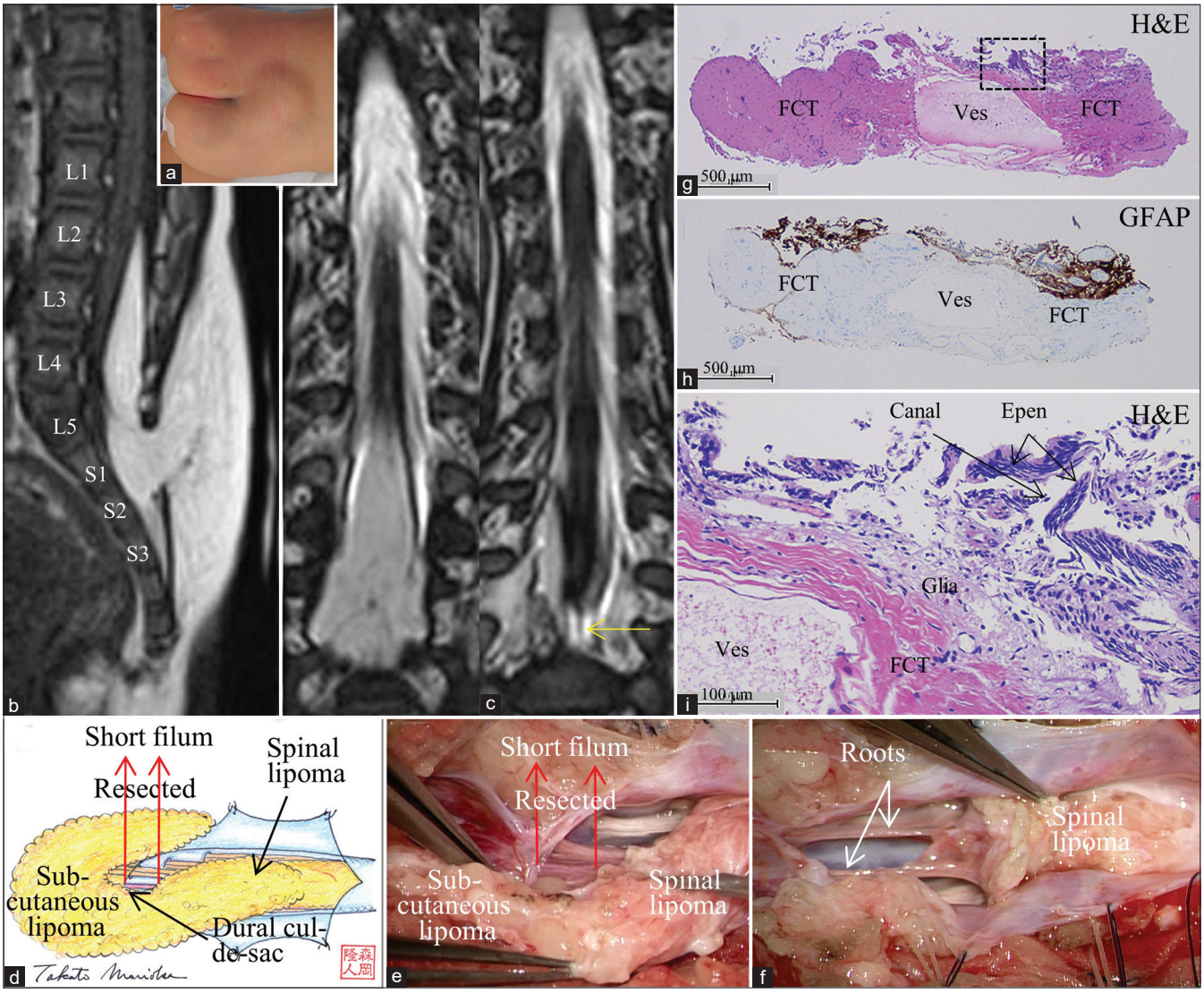


**Figure 2:** (Patient 2) (a) Photograph showing a subcutaneous lipoma at the lumbosacral region. Sagittal view of 3D-T1WI (slice thickness of 1.25 mm) (b) and serial coronal views of 3D-hT2WI (slice thickness of 1.25 mm) (c) depict a low-lying conus at the vertebral level of L3-4 that is tethered by the spinal lipoma of transitional type and short filum, which is barely seen (b-2, yellow arrow). Schematic drawings (d) and microscopic view of the operative findings (e and f). (d and e) With the dura opened, the subcutaneous lipoma is continuous with the spinal lipoma. Following untethering of the cord from the lipoma, the short filum (red arrows) is exposed, severed immediately rostral and caudal to the dural cul-de-sac and the spinal lipoma, respectively, and resected as column. (f) Following resection of the filum and debulking of the lipoma, the conus is slightly elevated, and spinal roots, which was involved with transitional lipoma, are stretched. (g-i) Photomicrograph of longitudinal sections of the filum stained with H and E (g and i) and immunostained for glial fibrillary acidic protein (h) A higher magnification view of the area indicated by the dotted square in (g) is shown in (i). In the marginal part of the fibrocollagenous tissue containing large vessel (ves), E-LC w/NGT is noted. No adipose tissue is observed.

In the present study, E-LC w/NGT was also noted in two out of six filar lipomas and in both TFTs. While E-LC w/NGT was reported to be present in the surgically resected filum associated with tethered cord syndrome[3,24] and even normal filum obtained at autopsy,[2] its embryological significance has not been fully discussed. In our previous study,[19] we showed that 13.9% of the patients with filar and caudal lipomas had E-LC w/NGT, while none of the patients with dorsal and transitional lipomas had E-LC w/NGT, suggesting that filar and caudal lipomas had the same embryological background as that of RMC during late secondary neurulation. The previous studies[7,18,20,21] also demonstrated that entities such as filar lipoma, TFT, and RMC can be considered members of a continuum of regression failure disorders occurring during late secondary neurulation. They speculated that they differ from each other in terms of timing and severity

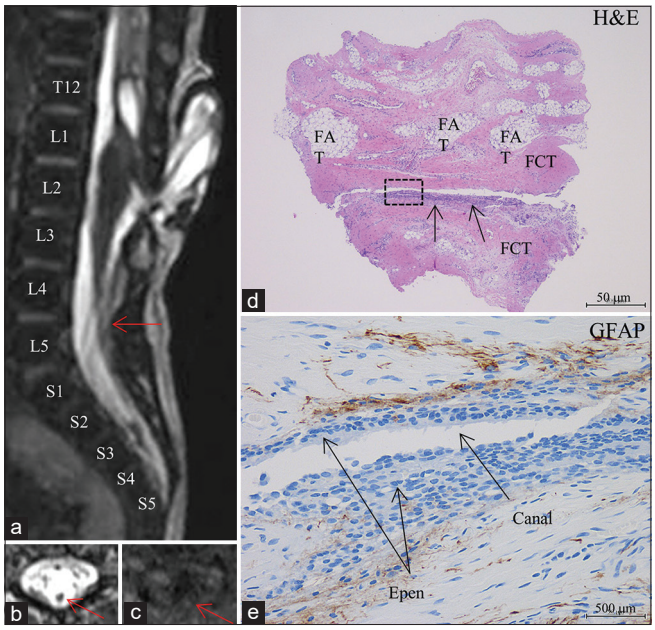


**Figure 3:** (Patient 9) (a) Sagittal view of 3D-hT2WI (slice thickness of 1.25 mm) depicts a low-lying conus at the vertebral level of L4-5 that is tethered by the stalk of limited dorsal myeloschisis (LDM), which starts at the dome of the meningocele sac, travels down in the sac, enters the spinal canal, and join the dorsal cord, and terminal filum of 1.5 mm in diameter. A syringomyelic cavity is noted immediately rostral to the cord LDM stalk attachment. This image is 1.25 mm lateral to the left side to the image in Figure 1b of our previous report.[9] (b and c) Axial views of T2WI (slice thickness of 2.60 mm) (b) and T1WI (slice thickness of 2.60 mm) (c) show that no lipomatous intensity is not noted in the terminal filum. (d and e) Photomicrograph of longitudinal sections of the resected filum stained with H and E (d) and immunostained for glial fibrillary acidic protein (e) A higher magnification view of the area indicated by the dotted square in (d) is shown in (e). E-LC w/NGT is noted in the fibrocollagenous tissue (FCT) with a small amount of FAT. The ratio of FAT to FCT is estimated to be 3:7

of apoptosis failure. Therefore, the histopathological coexistence of the E-LC w/NGT with filar lipoma and TFT demonstrated in this study, is not a surprising finding.[16,19-21] As the terminology for RMC, and lipoma and TFT was based on different backgrounds, namely, embryological and morphological backgrounds, respectively, it may be difficult in clinical practice to make a distinct diagnosis between these three entities.

Preoperative differential diagnosis is even more difficult. For example, it is generally accepted that differential diagnosis between the lipoma and TFT can be made from the intensity on preoperative T1-weighted MRI;[17] however, in this study, the ratio of fibroadipose and fibrocollagenous tissues was 3:7 or less, and the filum was demonstrated as isointense rather than hyperintense. It is also necessary to consider the possibility that the MRI signal abnormality site and the excised site of the filum do not always match. Thickened filum can be diagnosed when it has a diameter >2 mm;[17] however, the diameter of the TFT was <1.5 mm in this study. Furthermore, the diameter of the C-LS with RMC was <2 mm, probably depending on the age of the patient. We previously reported two cases with cystic RMC associated with terminal lipoma,[16] which was difficult to make a correct preoperative diagnosis. The more important issue is to diagnose the filar anomaly involved as an additional tethering tract and make an appropriate decision regarding untethering procedures.[4]

This study was a retrospective study with a small number of the patients. Although further studies with large numbers of patients are needed, this study revealed that E-LC w/NGT was noted not only in the two C-LS of RMCs but also in four fila with filar lipomas and TFTs. These findings provide further evidence for the idea that entities such as filar lipoma, TFT, and RMC can be considered consequences of a continuum of regression failure occurring during late secondary neurulation.

## CONCLUSION

Our findings provide further evidence for the idea that entities, such as filar lipoma, TFT, and RMC, can be considered consequences of a continuum of regression failure occurring during late secondary neurulation.

### Ethics statement

The authors confirm that written informed consent was obtained from the families of the infants described in this report.

The authors declare that this work complies with the guidelines for human studies, and the research was conducted ethically in accordance with the World Medical Association Declaration of Helsinki.

### Declaration of patient consent

The authors certify that they have obtained all appropriate patient consent.

### Financial support and sponsorship

Research Foundation of Fukuoka Children' Hospital.

### Conflicts of interest

There are no conflicts of interest.

## REFERENCES

1. Arai H, Sato K, Okuda O, Miyajima M, Hishii H, Nakanishi H, *et al.* Surgical experience of 120 patients with lumbosacral

lipomas. Acta Neurochir (Wien) 2001;143:857-64.
2. Choi BH, Kim RC, Suzuki M, Choe W. The ventriculus terminalis and filum terminate of the human spinal cord. Hum Pathol 2019;23:916-20.
3. Durdağ E, Börcek PB, Öcal Ö, Börcek AÖ, Emmez H, Baykaner MK. Pathological evaluation of the filum terminale tissue after surgical excision. Childs Nerv Syst 2015;31:759-63.
4. Gupta A, Rajshekhar V. Fatty filum terminale (FFT) as a secondary tethering element in children with closed spinal dysraphism. Childs Nerv Syst 2018;34:925-32.
5. Hashiguchi K, Morioka T, Fukui K, Miyagi Y, Mihara F, Yoshiura T, *et al*. Usefulness of constructive interference in steady-state magnetic resonance imaging in the presurgical examination for lumbosacral lipoma. J Neurosurg 2005;103:537-43.
6. Hiraoka A, Morioka T, Murakami N, Suzuki SO, Mizoguchi M. Limited dorsal myeloschisis with no extradural stalk linking to a flat skin lesion: A case report. Childs Nerv Syst 2018;34:2497-501.
7. Kim KH, Lee JY, Wang KC. Secondary neurulation defects-1: Retained medullary cord. J Korean Neurosurg Soc 2020;63:314-20.
8. Kurogi A, Murakami N, Morioka T, Mukae N, Shimogawa T, Kudo K, *et al*. Two cases of retained medullary cord running parallel to a terminal lipoma. Surg Neurol Int 2021;12:112.
9. Morioka T, Murakami N, Ichiyama M, Kusuda T, Suzuki SO. Congenital dermal sinus elements in each tethering stalk of coexisting thoracic limited dorsal myeloschisis and retained medullary cord. Pediatr Neurosurg 2020;55:380-7.
10. Morioka T, Murakami N, Kanata A, Tsukamoto E, Suzuki OS. Retained medullary cord associated with sacral subcutaneous meningocele and congenital dermal sinus. Childs Nerv Syst 2020;36:423-7.
11. Morioka T, Murakami N, Shimogawa T, Mukae N, Hashiguchi K, Suzuki SO, *et al*. Neurosurgical management and pathology of lumbosacral lipomas with tethered cord. Neuropathology 2017;37:385-92.
12. Morioka T, Murakami N, Yanagida H, Yamaguchi T, Noguchi Y, Takahata Y, *et al*. Terminal syringomyelia associated with lumbar limited dorsal myeloschisis. Childs Nerv Syst 2020;36:819-26.
13. Morioka T, Suzuki SO, Murakami N, Mukae N, Shimogawa T, Haruyama H, *et al*. Surgical histopathology of limited dorsal myeloschisis with flat skin lesion. Childs Nerv Syst 2019;35:119-28.
14. Morioka T, Suzuki SO, Murakami N, Shimogawa T, Mukae N, Inoha S, *et al*. Neurosurgical pathology of limited dorsal myeloschisis. Childs Nerv Syst 2018;34:293-303.
15. Morota N, Ihara S, Ogiwara H. New classification of spinal lipomas based on embryonic stage. J Neurosurg Pediatr 2017;19:428-39.
16. Mukae N, Morioka T, Suzuki SO, Murakami N, Shimogawa T, Kanata A, *et al*. Two cases of large filar cyst associated with terminal lipoma: Relationship with retained medullary cord. World Neurosug 2020;142:294-8.
17. Murakami N, Morioka T, Hashiguchi K, Yoshiura T, Hiwatashi K, Suzuki SO, *et al*. Usefulness of three-dimensional T1-weighted spoiled gradient-recalled echo and three-dimensional heavily T2-weighted images in preoperative evaluation of spinal dysraphism. Childs Nerv Syst 2013;29:1905-14.
18. Murakami N, Morioka T, Shimogawa T, Hashiguchi K, Mukae N, Uchihashi K, *et al*. Retained medullary cord extending to a sacral subcutaneous menigocele. Childs Nerv Syst 2018;34:527-33.
19. Murakami N, Morioka T, Shimogawa T, Mukae N, Inoha S, Sasaguri T, *et al*. Ependyma-lined canal with surrounding neuroglial tissues in lumboscaral lipomatous malformations: Relationship with retained medullary cord. Pediatr Neurosurg 2018;53:387-94.
20. Pang D, Chong S, Wang KC. Secondary neurulation defects-1: Thickened filum terminale, retained medullary cord. In: di Rocco C, Pang D, Rutka JT, editors. Textbook of Pediatric Neurosurgery. 1st ed. Switzerland: Springer; 2020.
21. Pang D, Zovickian J, Moes GS. Retained medullary cord in humans: Late arrest of secondary neurulation. Neurosurgery 2011;68:1500-19.
22. Pang D. Sacral agenesis and caudal spinal cord malformations. Neurosurgery 1993;32:755-79.
23. Sala F, Barone G, Tramontano V, Gallo P, Ghimenton C. Retained medullary cord confirmed by intraoperative neurophysiological mapping. Childs Nerv Syst 2014;30:1287-91.
24. Selçuki M, Vatansever S, Inan S, Erdemli E, Bağdatoğlu C, Polat A. Is a filum terminale with a normal appearance rarely normal? Childs Nerv Syst 2003;19:3-10.
25. Shirozu N, Morioka T, Inoha S, Imamoto N, Sasaguri T. Enlargement of sacral subcutaneous meningocele associated with retained medullary cord. Childs Nerv Syst 2018;34:1785-90.

**How to cite this article:** Morioka T, Murakami N, Suzuki SO, Mukae N, Shimogawa T, Kurogi A, *et al*. Surgical histopathology of a filar anomaly as an additional tethering element associated with closed spinal dysraphism of primary neurulation failure. Surg Neurol Int 2021;12:373.